Journal of Visualized Experiments

Stereocilia Bundle Imaging with Nanoscale Resolution in Live Mammalian Auditory Hair Cells
--Manuscript Draft--

Question	Response
Please specify the section of the submitted manuscript.	Neuroscience
Please indicate whether this article will be Standard Access or Open Access.	Standard Access (US$2,400)
Please indicate the **city, state/province, and country** where this article will be **filmed**. Please do not use abbreviations.	Lexington, KY, USA
Please confirm that you have read and agree to the terms and conditions of the author license agreement that applies below:	I agree to the Author License Agreement
Please provide any comments to the journal here.	

1 **TITLE:**
2 Stereocilia Bundle Imaging with Nanoscale Resolution in Live Mammalian Auditory Hair Cells
3
4 **AUTHORS AND AFFILIATIONS:**
5 Carolina Galeano-Naranjo[1,2], A. Catalina Veléz-Ortega[1] , Gregory I. Frolenkov[1]
6
7 [1]Department of Physiology, College of Medicine, University of Kentucky, Lexington, KY 40536-
8 0298, USA.
9 [2]Universidad Nacional de Colombia, Medellin, Antioquia, Colombia.
10
11 Corresponding authors:
12 Gregory I. Frolenkov   (gregory.frolenkov@uky.edu)
13 A. Catalina Veléz-Ortega   (catavelezo@uky.edu)
14
15 Email addresses of Co-Authors:
16 Carolina Galeano-Naranjo (carolina.galeano.naranjo@uky.edu)
17 A. Catalina Veléz-Ortega (catavelezo@uky.edu)
18 Gregory I. Frolenkov (gregory.frolenkov@uky.edu)
19
23
24 **SUMMARY:**
25 Here we present a protocol for the Hopping Probe Ion Conductance Microscopy (HPICM), a non-
26 contact scanning probe technique that allows nanoscale imaging of stereocilia bundles in live
27 auditory hair cells.
28
29 **ABSTRACT:**
30 Inner ear hair cells detect sound-induced displacements and transduce these stimuli into
31 electrical signals in a hair bundle that consists of stereocilia that are arranged in rows of
32 increasing height. When stereocilia are deflected, they tug on tiny (~5 nm in diameter)
33 extracellular tip links interconnecting stereocilia, which convey forces to the mechanosensitive
34 transduction channels. Although mechanotransduction has been studied in live hair cells for
35 decades, the functionally important ultrastructural details of the mechanotransduction
36 machinery at the tips of stereocilia (such as tip link dynamics or transduction-dependent
37 stereocilia remodeling) can still be studied only in dead cells with electron microscopy.
38 Theoretically, scanning probe techniques, such as atomic force microscopy, have enough
39 resolution to visualize the surface of stereocilia. However, independent of imaging mode, even
40 the slightest contact of the atomic force microscopy probe with the stereocilia bundle usually
41 damages the bundle. Here we present a detailed protocol for the hopping probe ion conductance
42 microscopy (HPICM) imaging of live rodent auditory hair cells. This non-contact scanning probe
43 technique allows time lapse imaging of the surface of live cells with a complex topography, like
44 hair cells, with a single nanometers resolution and without making physical contact with the

45 sample. The HPICM uses an electrical current passing through the glass nanopipette to detect
46 the cell surface in close vicinity to the pipette, while a 3D-positioning piezoelectric system scans
47 the surface and generates its image. With HPICM, we were able to image stereocilia bundles and
48 the links interconnecting stereocilia in live auditory hair cells for several hours without noticeable
49 damage. We anticipate that the use of HPICM will allow direct exploration of ultrastructural
50 changes in the stereocilia of live hair cells for better understanding of their function.
51
52 **INTRODUCTION:**
53 Despite the fact that stereocilia bundles in the auditory hair cells are big enough to be visualized
54 by optical microscopy and deflected in live cells in a patch clamp experiment, the essential
55 structural components of the transduction machinery such as tip links could be imaged only with
56 the electron microscopy in dead cells. In the mammalian auditory hair cells, the transduction
57 machinery is located at the lower ends of the tip links, i.e., at the tips of the shorter row
58 stereocilia[1] and regulated locally through the signaling at the tips of stereocilia[2,3]. Yet, label-free
59 imaging of the surface structures at this location in live hair cells is not possible due to the small
60 sizes of stereocilia.
61
62 The mammalian cochlea has two types of auditory sensory cells: inner and outer hair cells. In the
63 inner hair cells, stereocilia are longer and thicker compared to those in the outer hair cells[4]. The
64 first and second row of stereocilia have a diameter of 300-500 nm in mouse or rat inner hair cells.
65 Due to the diffraction of light, the maximum resolution achievable with a label-free optical
66 microscopy is approximately 200 nm. Hence, visualization of individual stereocilia within first and
67 second rows of the inner hair cell bundle is relatively easily with optical microscopy. In contrast,
68 shorter row stereocilia in the inner hair cells and all stereocilia of the outer hair cells have
69 diameters around 100-200 nm and cannot be visualized with optical microscopy[5]. Despite recent
70 progress in super-resolution imaging, this fundamental limitation persists in any optical label-free
71 imaging. All current commercially available super-resolution techniques do require some sort of
72 fluorescent molecules[6], which limits their applications. In addition to limitations due to the need
73 for specific fluorescently tagged molecules, exposure to intense light irradiation has been shown
74 to induce cellular damage and might influence cellular processes, which is a great disadvantage
75 when studying live cells[7].
76
77 Our current knowledge of the ultrastructural details of hair cell stereocilia bundles has been
78 obtained mostly with various electron microscopy (EM) techniques, such as scanning electron
79 microscopy (SEM), transmission electron microscopy (TEM), freeze-fracture EM, and recently
80 with 3D techniques such as serial sectioning with focused ion beam or cryo-EM tomography[8-16].
81 Unfortunately, all these EM techniques require chemical or cryofixation of the sample.
82 Depending on the time scale of the phenomena, this requirement makes a study of the dynamic
83 processes at the tips of stereocilia either impossible or very labor intensive.
84
85 Limited efforts have been made to image hair bundles of live hair cells with atomic force
86 microscopy (AFM) [17,18]. Since AFM operates in physiological solutions, it could, in theory, visualize
87 dynamic changes in the stereocilia bundles of live hair cells over time. The problem lies in the
88 principles of high-resolution AFM, which implies certain physical contact between the AFM probe

89   and the sample, even in the least damaging "tapping" mode[19]. When the AFM probe encounters
90   a stereocilium, it usually crashes against it, damaging the structure of the hair bundle. As a result,
91   this technique is not suitable for visualizing live, or even fixed, hair cells bundles[17,18]. The problem
92   may be partially alleviated by using a large ball-shaped AFM probe that imposes only
93   hydrodynamic forces to the surface of the sample[20]. However, even though such a probe is ideally
94   suited to test mechanical properties of the sample[21], it provides only a sub-micrometer resolution
95   when imaging the organ of Corti[22] and still applies to the sample a force that may be substantial
96   for the highly sensitive stereocilia bundles.
97
98   Scanning ion conductance microscopy (SICM) is a version of scanning probe microscopy that uses
99   a glass pipette probe filled with a conductive solution[23]. SICM detects the surface when the
100 pipette approaches the cell and the electric current through the pipette decreases. Since this is
101 happening well before touching the cell, the SICM is ideally suited for non-contact imaging of live
102 cells in physiological solution[24]. The best resolution of SICM is on the order of single nanometers,
103 which allows resolving individual protein complexes at the plasma membrane of a living cell[25].
104 However, similar to other scanning probe techniques, SICM is able to image only relatively flat
105 surfaces. We overcame this limitation by inventing hopping probe ion conductance microscope
106 (HPICM)[26], in which the nanopipette approaches the sample at each imaging point (**Figure 1A**).
107 Using HPICM, we were able to image stereocilia bundles in live auditory hair cells with nanoscale
108 resolution[27].
109
110 Another fundamental advantage of this technique is that HPICM is not only an imaging tool. In
111 contrast to other scanning probe techniques, the HPICM/SICM probe is an electrode widely used
112 in cell physiology for electrical recordings and local delivery of various stimuli. Ion channel activity
113 does not usually interfere with HPICM imaging, because the total current through the HPICM
114 probe is several orders of magnitude larger than the extracellular current generated by the
115 largest ion channels[25]. However, HPICM allows precise positioning of the nanopipette over a
116 structure of interest and subsequent single-channel patch-clamp recording from this structure[28].
117 This is how we obtained the first preliminary recordings of single channel activity at the tips of
118 the outer hair cell stereocilia[29]. It is worth mentioning that even a large current through the
119 nanopipette cannot produce significant changes of the potential across the plasma membrane
120 due to enormous electrical shunt of the extracellular medium. However, individual ion channels
121 can be activated mechanically by flow of liquid through the nanopipette[30] or chemically by local
122 application of an agonist[31].
123
124 In HPICM, the image is generated when a nanopipette sequentially approaches the sample at
125 one point, retracts, and then moves in lateral direction to repeat the approach (**Figure 1A**). A
126 patch clamp amplifier constantly applies voltage to an AgCl wire in the pipette (**Figure 1B**) to
127 generate a current of ~1 nA in the bath solution. The value of this current when the pipette is
128 away from the surface of the cell is determined as a reference current (I_{ref}, **Figure 1C**). Then, the
129 pipette moves in the Z axis to approach the sample until the current is reduced by an amount
130 predefined by the user (setpoint), usually 0.2%-1% of the I_{ref} (**Figure 1C**, top trace). The system
131 then saves Z value at this moment as the height of the sample, together with X and Y coordinates
132 of this imaging point. Then, the pipette is retracted away from the surface (**Figure 1C**, bottom

133 trace) at a speed defined by the user, usually 70-90 nm/ms. After retraction, the pipette (or, in
134 our case, the sample – see **Figure 1B**) is moved laterally to the next imaging point, a new
135 reference current value is obtained, and the pipette once again approaches the sample, repeating
136 the process. The X-Y movement of the pipette is preferred in an upright microscope setup that is
137 typically used for recordings of the hair cell mechanotransduction currents. In this setting, the
138 HPICM probe approaches the hair cell bundles not from the top but at an angle[32]. However, the
139 best resolution of HPICM imaging is achieved in an inverted microscope setup (**Figure 1A,B**),
140 where the movement of the sample in X-Y directions is de-coupled from Z-movement of the
141 nanopipette, thereby eliminating potential mechanical artefacts.
142
143 Using HPICM, we obtained topographic images of mouse and rat inner and outer hair cell
144 stereocilia bundles, and even visualized the links between the stereocilia that are about 5 nm in
145 diameter[26,27]. The success of hair cell bundle imaging with this technique relies on several factors.
146 First, the noise (variance) of the nanopipette current should be as small as possible to allow the
147 lowest possible setpoint for HPICM imaging. A low setpoint allows HPICM probe to "sense"
148 stereocilia surface at a larger distance and at any angle to the probe approach and, surprisingly,
149 improves X-Y resolution of HPICM imaging (see **Discussion**). Second, the vibrations and drifts in
150 the system should be decreased to less than 10 nm, since they contribute directly to the imaging
151 artefacts. Finally, even though the HPICM probe and the specimen stage are moved in Z and X-Y
152 axes by the calibrated feedback-controlled piezo actuators that have an accuracy of a single
153 nanometer or better, the diameter of the nanopipette tip determines the spread of the current
154 (sensing volume) and hence the resolution (**Figure 1A**). Therefore, before imaging live hair cells,
155 it is vital to pull the adequate pipettes, reach the desired resolution with calibration samples, and
156 achieve low noise in the recording system.
157
158 For at least a couple of decades, the SICM technique has not been commercially available and it
159 has been developing by only few labs in the world with the leading lab of Prof. Korchev in the
160 Imperial College (UK). Recently, several SICM systems became commercially available (see **Table
161 of Materials**), all of which are based on the original HPICM principles. However, imaging
162 stereocilia bundles in the hair cells requires several custom modifications that are technically
163 challenging (or even impossible) in the closed "ready-to-go" systems. Therefore, some
164 component integration is needed. Since HPICM setup represents a patch clamp rig with more
165 stringent vibration and drift requirements and a piezo-driven movement of the HPICM probe and
166 the sample (**Figure 1D**), this integration is relatively easy for any researcher, who is proficient in
167 patch clamping. However, a scientist without proper background would definitely need some
168 training in electrophysiology first. Despite remaining challenges such as increasing the speed of
169 imaging (see **Discussion**), we have been able to image stereocilia bundles in live hair cells with
170 nanoscale resolution without damaging them.
171
172 This paper presents a detailed protocol to perform successful HPICM imaging of the live auditory
173 hair cell bundles in young postnatal rat or mouse cochlear explants using our custom system. The
174 integrated components are listed in the **Table of Materials**. The paper also describes common
175 problems that can be encountered and how to troubleshoot them.
176

PROTOCOL:

The study was performed in accordance with the recommendations in the Guide for the Care and Use of Laboratory Animals of the National Institutes of Health. All animal procedures were approved by the Institutional Animal Care and Use Committee (IACUC) at the University of Kentucky (protocol 00903M2005).

1.   Manufacturing and testing the nanopipettes

1.1   Create a program in the micropipette puller to obtain pipettes with a resistance between 200 and 400 MΩ, which corresponds to inner tip diameters of approximately 50-70 nm. The parameters will depend on the micropipette puller. To obtain short pipettes with non-flexible fine tips, check in the operational manual of the puller.

1.2   Use borosilicate glass capillaries with outer/inner diameters of 1/0.58 mm and an inner filament to facilitate filling. The length of the pipette is crucial because it determines the frequency of the lateral mechanical resonance of the pipette. The longer is the pipette, the lower is the resonant frequency and the harder is to avoid this resonance.

NOTE: The user should try to manufacture the shortest pipette the holder can accept. The length of nanopipettes in this experiment is usually 15-25 mm (**Figure 2A**).

1.3   Fill the nanopipette up to its middle point (**Figure 2A**) with a bath solution, either Leibovitz's L-15 or with Hank's Balanced Salt Solution (HBSS) supplemented with 20 mM D-glucose (to adjust osmolarity). To avoid potential artefacts, use the same solution that will be used in the bath for recordings.

1.4   Using an optical microscope with a magnification of 10x, check for any bubbles at the tip of the pipette (**Figure 2B**). The bubbles would prevent the current flow. It is harder to remove bubbles in the pipettes that have been pulled several hours before the experiment. Therefore, it is recommended to pull new pipettes with every experiment.

1.5   Once the pipette is free of bubbles, mount it in the HPICM pipette holder (**Figure 2C**).

1.6   Place the sample (tissue or calibration standard) on the custom-build chamber and add 4 mL of the above-mentioned bath solution.

1.7   Place a custom-build chamber on the HPICM stage and introduce the ground electrode in the solution.

1.8   Make sure that the voltage being applied to the pipette by the patch clamp amplifier is zero.

218

219   1.9   Move the pipette in Z until it touches the liquid.

220

221   1.10   Set the amplifier offset to zero and then add +100 mV to check the pipette current.

222

223   1.11   Calculate the resistance and the diameter of the pipette, based on Ohm's law:

$$R = \frac{V}{I}$$

225   where R is the resistance (MΩ), V is the voltage applied to the nanopipette (mV) and I is the
226   current flowing through the nanopipette (nA).

227

228   1.11.1. Calculate the inner diameter of the pipette as described elsewhere according to the
229   following formula[12]:

$$ID_{Tip} = \frac{1000}{\sqrt{R}}$$

231

232   NOTE: The ideal resistance value is between 200 and 400 MΩ. Pipettes with a resistance higher
233   than 400 MΩ might lead to an unstable current due to their small size (< 50 nm inner diameter).
234   On the contrary, pipettes with resistances smaller than 200 MΩ are too large (> 70 nm inner
235   diameter) and would not resolve small features. Its recommended to start imaging with the
236   pipettes of 200 MΩ resistance, as they are easier to manufacture and tend to provide less
237   electrical noise.

238

239   **2.   Minimizing sample drifts and vibrations**

240

241   NOTE: To decrease the mechanical noise in the system during imaging, mount the samples on
242   the custom-built chambers that utilize thick glass slides (~1.2 mm):

243

244   2.1   Remove the glass portion off a 50 mm glass-bottom dish, leaving the plastic walls intact.

245

246   2.2   Glue the plastic portion of the cell culture dish on top of the thick glass slide with silicon
247   glue.

248

249   2.3   Mount the calibration sample in the middle of the chamber (on top of the glass slide)
250   using either silicon glue or thin double-sided tape.

251

252   2.4   Firmly secure the chamber onto the HPICM stage using double-sided tape.

253

254   2.5   During imaging, close the Faraday cage and cover it with a blanket to minimize electrical
255   interference and thermal drift, correspondingly.

256

257   **3.   Testing the resolution with AFM calibration standards**

258

259   NOTE: It is strongly recommended to image AFM standards (see **Table of Materials**) before

260 imaging live cells in order to troubleshoot the system and test its resolution in the X-Z-Y axes. The
261 calibration standards have silicon dioxide pillars and holes of different shapes but fixed
262 heights/depths (i.e., 20 or 100 nm) on a 5 x 5 mm silicon chip. Starting with the 100 nm calibration
263 standard is recommended, to guarantee that the Z resolution is below 100 nm. After achieving a
264 successful high-resolution image of the pillars or holes in this calibration sample (**Figure 3A**),
265 move to the 20 nm standard. If the imaging of the latter standard is successful (**Figure 3B**), the
266 resolution in the Z axis is guaranteed to be below 20 nm and appropriate for the imaging of the
267 hair cell stereocilia bundles[12]. The following steps are used to image both calibration standards.

269 3.1   Attach the calibration standard to the chamber with silicon glue.

271 3.2   Add 4 mL of HBSS to the chamber to cover the calibration sample. Then, secure the
272 chamber to the XY stage of the HPICM setup using double-sided tape.

274 3.3   Clamp the magnetic holder of the ground electrode to the stage near the chamber and
275 immerse the electrode into the bath solution (**Figure 1B**).

277 3.4   Mount the nanopipette into the holder, immerse it into the batch solution, and set its
278 current to ~1 nA following the steps described in Section 1.

280 3.5   Position the nanopipette approximately above the center of the calibration standard
281 using a course patch-clamp manipulator. Visual inspection is usually enough for this positioning,
282 since the area covered by silicon dioxide structures is relatively large (1 x 1 mm). In contrast to
283 the organ of Corti explants (see below), calibration standard is non-transparent and, therefore, a
284 more precise positioning guided by optical imaging is not possible for this sample.

286 3.6   Increase the setpoint while monitoring the signal from the sensor of the Z piezo actuator
287 on an oscilloscope in a real time. After establishing a stable repeatable Z approach cycle (as in
288 **Figure 1C**, bottom), decrease the setpoint to the value that is just above the point of instability.
289 This procedure would ensure the optimal setpoint for this particular nanopipette.

291 3.7   Move the pipette down at a speed of ~5 μm/s with a patch clamp micromanipulator until
292 it reaches the sample. At this moment, the bottom level of the real-time Z positioning signal
293 (**Figure 1C**) will increase, indicating that the nanopipette is withdrawn due to "sensing" the
294 sample surface. Any further movement of the nanopipette will result in further positive shift of
295 Z-positioning signal.

297 NOTE: Be careful not to exceed the upper limit of Z piezo actuator movement.

299 3.8   Start imaging at low resolution (see **Table 1**). Due to uneven mounting of the AFM
300 standard, the highest point of the area of interest may be unknown. Therefore, set the amplitude
301 of pipette retraction (hop amplitude) to at least 200-500 nm.

303 3.8.1   Once the highest point of the sample in the imaging area is identified, decrease the hop

4   Making custom-built chambers to secure the cochlear explants

NOTE: Mount the cochlear explants in the chambers with custom-built clamping systems that
utilize either flexible glass pipettes (step 4.1) (**Figure 4A**) or dental floss (step 4.2) (**Figure 4B**). The
glass pipette chamber could be sterilized and used for the cultured organs of Corti, while dental
floss chamber provides a more secure holding of the sample and a control over stereocilia bundle
orientation during mounting. These custom-built chambers need to be prepared in advance, but
they can be cleaned and re-used in several imaging sessions.

4.1   Make a chamber using flexible glass pipettes

4.1.1 Pull two thin and flexible glass fibers from glass capillaries using a pipette puller. Our pulled
glass fibers typically measure 1 to 2 cm in length and are fairly flexible.

4.1.2 Place a small drop of the silicone elastomer on top of a glass coverslip. Use coverslips of 2
cm in diameter.

4.1.3 Place the ends of two glass fibers on the silicone drop and arrange the fibers to have a small
degree of separation between them (**Figure 4A**).

4.1.4 Place the coverslip on a hot plate to quickly cure the elastomer (1 to 3 min).

4.1.5 Glue the coverslip onto the glass bottom of the chamber described in Section 2 using a small
amount (1-3 μL) of silicone elastomer and allowing it to cure overnight.

4.2 Making a chamber using dental floss:

4.2.1 Remove the glass portion of a 50 mm glass-bottom dish, leaving the plastic walls intact.
Then glue the plastic portion of the cell culture dish on top of a 1.2 mm thick glass slide with
silicon glue.

4.2.2 Mount one plastic coverslip (6.5 x 6.5 mm) with the same glue to the center of the chamber.
Then repeat the process with another coverslip on top of the previous one.

348

349   4.2.3 Mount two small tungsten or gold-plated wires (12 mm of length and ~0.5 mm in diameter)
350   with silicon glue, each one at opposites sides of the cover slides. Glue them far enough (> 10-15
351   mm) from the cover slides (**Figure 4B**).

352

353   4.2.4 Separate two dental floss strands and place them on top of the cover slides and secure
354   them to the wires by making a knot. Leave a small gap between both strands (**Figure 4B**, short
355   arrows).

356

357   4.3 Clean the chambers after every use

358

359   4.3.1 Gently remove the tissue from the chamber using fine tweezers and lightly scrape any tissue
360   residues left behind.

361

362   4.3.2 Rinse the chamber first with 70% ethanol and then with distilled water.

363

364   4.3.3 Repeat the rinse cycle if needed.

365

366   4.3.4 Place the chamber upside down on a filter paper to let it dry until next experiment. The
367   chambers do not need to be sterilized, unless culturing of the organ of Corti is planned after the
368   imaging.

369

370   **5   Dissecting the rodent organ of Corti**

371

372   5.1. Perform dissection of the young postnatal cochlear explants as described in detail
373   elsewhere[13].

374

375   5.2. For HPICM imaging, dissect the organ of Corti from mice between postnatal days 3 and 6 (P3-
376   6), and from rats between postnatal days 3 and 8 (P3-8).

377

378   NOTE: Older hair cells are more susceptible to the damage during dissection and, therefore,
379   cannot be used for hours-long time lapse HPICM imaging.

380

381   5.3. Do not forget to remove the tectorial membrane before HPICM imaging.

382

383   5.4. Immediately after dissection, secure the tissue in one of the chambers described in Section
384   4, either placing it under the flexible glass pipettes or under the two dental floss strands (**Figure
385   4**). Pre-fill these chambers with 4 mL of the room temperature bath solution (to minimize bubble
386   formation).

387

6 Imaging of the auditory hair cells

6.1 Mount the chamber with a freshly isolated organ of Corti on the X-Y piezo stage using double-sided tape and make sure that it is firmly secured to minimize chamber drift in X and Y axes (**Figure 1B**).

6.2 Follow steps in Section 1 to place a new nanopipette and check for the correct pipette resistance.

6.3 Using patch clamp micromanipulator, position nanopipette over the hair cell region, while observing the organ of Corti explant in an inverted microscope.

6.4 Check if the system is stable with a setpoint of 0.5% or lower by recording the real-time current and Z positioning signal on the oscilloscope (as in **Figure 1C**). If Z signal is not stable, try to decrease the cutoff frequency of the low-pass filter of the patch clamp amplifier. However, it cannot be lower than the response time of Z piezo actuator (to avoid pipette collision with the sample due to delayed current readings).

NOTE: In practice, 5 kHz setting of this filter is found to be optimal. It is better to replace the nanopipette, if Z-signal is still unstable.

6.5 Once a stable a stable recording is achieved, determine the optimal setpoint and approach the sample with HPICM pipette as described in the steps 3.6-3.7 above.

6.6 First, perform low resolution imaging (see **Table 1**), using a hop amplitude of at least 6 to 8 μm. To image tall structures such as the hair cell stereocilia bundles, make sure that the hop amplitude is enough to avoid collision with these structures.

NOTE: If the hop amplitude is not enough, the pipette will not be able to jump over a stereocilium and there will be an imminent collision. The collision of the HPICM probe with a stereocilium may damage the hair bundle. Therefore, in cases when the height of the stereocilia bundle is uncertain, use a bigger hop amplitude.

6.7 Get familiar with the topography of the organ of Corti by first performing and/or studying images obtained with scanning electron microscopy (**Figure 5**).

NOTE: If the HPICM image is uniform with the heights smaller than 1 μm in every imaging point, the pipette is likely scanning the glass bottom and not the tissue. Alternatively, the pipette may "land" on a different region of the cochlear explant, away from the hair cells.

6.8 If the pipette needs to be moved to a new X-Y location, retract it about 500 nm to avoid collisions with any tall features within the tissue. Repeat low-resolution HPICM imaging until the region of interest with the hair cells is found.

431

444

445 **7   Image processing**

446

447 NOTE: Imaging artefacts are common in HPICM imaging. Some of them can be corrected by image
448 acquisition parameters, while others require post-processing either with a specialized SICM
449 viewer or with more general data-processing programs like ImageJ or MatLab. Here we describe
450 the most common artefacts and how we fix them with SICM viewer.

451

452 7.1   Perform slope correction

453

454 NOTE: It is not obvious for a beginner, but human eye cannot resolve sub-micrometer size
455 features at the surface of a cell, if the imaging area has an overall slope of equal or larger size
456 (**Figure 3A,B**, left). Therefore, it is necessary to determine the average slope of an imaged area
457 (by fitting HPICM 3D image data to a single plane) and subtract it from the HPICM image (**Figure
458 3A,B,** middle).

459

460 7.1.1   Click **Open** to open an image with SICM viewer.

461

462 7.1.2   Select the **Image Correction** tab.

463

464 7.1.3   Select the **Correct Slope** tab.

465

466 7.1.4   Press the **Correct Slope** button for an automated slope correction.

467

468 7.2   Perform line alignment

469

470 NOTE: As mentioned before, mechanical and/or thermal drifts as well as cell movement artefacts
471 represent a significant problem in HPICM imaging. A small drift with a speed of less than a
472 micrometer per minute is usually not noticeable in a regular patch clamp setup. Yet, it could
473 produce artefacts of several tens of nanometers in HPICM imaging, which is significantly larger
474 than the resolution of HPICM. Therefore, it is not uncommon to encounter sudden jumps in Z

475 axis between two neighboring HPICM scan lines during imaging. This could be corrected by
476 analyzing differences between starting (and/or ending) Z-values in these neighboring scan lines.
477
478 7.2.1 Click **Open** to open an image with SICM viewer.
479
480 7.2.2 Select the **Image Correction** tab.
481
482 7.2.3 Select the **Correct Slope** tab.
483
484 7.2.4 Choose the width of lines to be aligned. Press on the button **ButtonDestripeLineFit** for an
485 automated line alignment correction.
486
487 7.3 Perform noise reduction
488
489 NOTE: While obtaining images with HPICM, small fluctuations in the nanopipette current can lead
490 to the nanopipette stopping far from the surface of the sample, especially with low setpoints. It
491 results in the appearance of small white dots in the image. In order to correct this imaging
492 artefact, it is necessary to identify the imaging points with the Z-value significantly larger than
493 that of the neighbors and replace this value with an average of the neighbors. This is be done by
494 an adjustable median filter.
495
496 7.3.1 Click **Open** to open an image with SICM viewer.
497
498 7.3.2 Select the **Image Processing** tab.
499
500 7.3.3 Select the **Noise reduction** tab.
501
502 7.3.4 Set the **Threshold filter** (μm) for the pixels to be removed.
503
504 **REPRESENTATIVE RESULTS:**
505 The protocol presented in this paper can be used to visualize any live cells with complex
506 topography. Following these steps, we routinely obtain images of live rat auditory hair cell
507 bundles (**Figure 6B,D**). In spite of having lower X-Y resolution when compared to SEM images,
508 our HPICM images can successfully resolve the different rows of stereocilia, the shape of the
509 stereocilia tips, and even the small links (~5 nm in diameter) connecting adjacent stereocilia
510 (**Figure 6F**). In addition, HPICM images have information in 3D that SEM images lack. Given the
511 non-contact nature of this type of imaging technique, we were also able to perform continuous
512 time-lapse HPICM imaging of the same hair cell bundle for several hours (i.e., 5-6 h regularly)
513 without damaging the bundle cohesiveness (**Figure 7**). Thus, HPICM exhibits a great potential for
514 the study of dynamic structural changes of the hair cell bundles over time.
515
516 Although we provide several ranges for pipette size, current setpoint, low- and high-resolution
517 parameters, and hop amplitudes, each user might need to slightly optimize their settings to
518 obtain successful HPICM images of live hair cell bundles. Smaller setpoints produce better quality

519　images. However, with a very low setpoint, the system might interpret small fluctuations in the
520　current as encountering the cell surface and this will lead to the "white dot" noise in the image
521　(**Figure 8A**). Similarly, large hop amplitudes might increase the lateral resonance of the pipette
522　and also produce noisy pixels (**Figure 8B**). In contrast, if the hop amplitude is too small or the
523　setpoint is too high, the nanopipette might collide with the sample and lead to imaging artefacts
524　or even damage the hair bundle (**Figure 8C,D**). We recommend performing the imaging at lower
525　resolution while tweaking all these parameters to minimize damage to the sample or to the
526　nanopipette.
527
528　**FIGURE AND TABLE LEGENDS:**
529
530　**Figure 1: Principles of hopping probe ion conductance microscopy (HPICM).** (**A**) An electric
531　current passing through the nanopipette generates a "sensing volume" at the tip of the pipette.
532　To image complex structures like the hair cell stereocilia bundles, the pipette approaches toward
533　the cell surface from above and retracts after detecting the surface. After a lateral move at each
534　step, the pipette continues to "hop" above the sample generating the image of the cell. Notice
535　that the hop amplitude must be sufficient for the pipette to "climb" to a stereocilium. Illustrated
536　hop amplitude would work for left-to-right scanning (from smallest to a tallest stereocilium,
537　indicated by an arrow). However, it is too small for right-to-left scanning when the pipette meets
538　the tallest stereocilium first. (**B**) Experimental setup. A custom-made chamber with the organ of
539　Corti explant is mounted on a XY nanopositioning stage with an aperture for optical microscopy
540　observation. The nanopipette is moved by a separate ultra-fast Z piezo actuator. To position the
541　nanopipette over the region of interest, Z actuator is mounted on a conventional
542　micromanipulator (not shown) together with the patch clamp *amplifier headstage*. *Ground*
543　*electrode* is mounted on a magnetic holder and inserted into the bath. (**C**) Representative
544　recordings of the pipette current (*top* trace) and Z position of the pipette (bottom trace) during
545　imaging. When the pipette is away from the cell surface, the reference value of the current
546　passing through the pipette is determined (I_{ref}). Then, the pipette is moved toward the sample
547　(approach). When the "sensing volume" meets the cell surface, the pipette current starts
548　decreasing. The command for withdrawal is issued when the current decrease reaches a setpoint,
549　which is typically 0.2% - 1% of I_{ref}. (**D**) Schematics of the equipment that need to be added to a
550　conventional patch clamp setup for HPICM imaging. A dedicated patch clamp amplifier records
551　the nanopipette current (I) that is used by SICM controller in HPICM mode to generate command
552　signals to X, Y, and Z axes. Instrum*entation amplifier* provides offset, scaling, and low pass filtering
553　to these signals, if needed. Unfortunately, X/Y/Z signals from the controller cannot be applied
554　directly to the piezo actuators due to large errors caused by hysteresis and creeping that are
555　inherent to piezo ceramic. Therefore, each *piezo actuator* (*translation stage*) has a build-in
556　motion *sensor* that sends feedback signal to the proportional-integral-derivative (PID) controller
557　that pre-shapes the command signal to correct for these errors. Note that relatively slow X and
558　Y axes could use *PID controllers* that are built in the *piezo amplifier*, while a faster Z axis requires
559　a dedicated fast *PID controller*.
560
561　**Figure 2: Nanopipette fabrication and filling.** (**A**) An approximately 2 cm-long nanopipette filled
562　with the intrapipette solution (HBSS). (**B**) An image of the bubble (arrow) that is typically formed

after filling the pipette. The bubble usually moves away within few minutes of microscope illumination (an LCD digital microscope at 10x). (**C**) A nanopipette mounted into the SICM head. The arrow points to the AgCl electrode inside the pipette. Notice that the pipette holder is silver painted and grounded to minimize radiative electrical pickup from the Z piezo actuator.

Figure 3: Imaging of AFM calibration standards to determine adequate stability, vibration isolation, and electrical noise in the system. (**A**) Raw (left), post-processed (middle), and 3D (right) images of the HS-100MG calibration standard. The surface profile of the standard is shown schematically at the top. Since the standard is never aligned perfectly perpendicular to the nanopipette, the post-processing slope correction is needed to reveal small vertical features of the sample. (**B**) Similar raw (left), post-processed (middle), and 3D (right) images of the HS-20MG calibration standard that has smaller, 20-nm deep indentations. Note that greyscale of a pixel in an HPICM image indicates the height of the sample at that point.

Figure 4: Mounting of the organ of Corti explant. (**A**) The explant is held by two glass pipettes that are glued to the glass-bottom Petri dish. (**B**) The explant is secured by two dental floss strands (arrows) in a custom-made imaging chamber. Inset shows magnified image of the organ of Corti.

Figure 5: Navigation of the HPICM probe to the hair cell region. (**A**) SEM image of the cochlear explant showing rows of inner (IHCs) and outer (OHCs) hair cells and distinct types of supporting cells. (**B**) Representative HPICM image of the cells in Kolliker's organ. (**C**) An HPICM image of the Hensen's cells. Note that these two types of supporting cells have very distinct shapes, which helps determining whether the HPICM probe landed to an area that is radial or peripheral to the hair cells.

Figure 6: Comparison between scanning electron microscopy (SEM) and hopping probe ion conductance microscopy (HPICM) imaging of stereocilia bundles in young postnatal rodent inner hair cells. (**A,C**) SEM images provide sub-nanometer resolution of the surface details but in the cells that are fixed and shrunk due to critical point drying. In addition, SEM images do not allow 3D analysis. (**B,D**) HPICM images (left) have a worse resolution (~5-10 nm) but they are obtained in live cells, allow time lapse imaging, and carry information on exact heights, which allows 3D reconstruction and measurements (right). (**E,F**) Extracellular links between stereocilia are evident in both SEM (**E**) and HPICM (**F**) images (arrows). Cell ages: A, postnatal day 5 (P5) mouse; B, P6 rat; C, P8 mouse; D, P5 rat; E, P7 mouse; and F, P5 rat. In all HPICM images, greyscale of a pixel indicates the height of the sample at that point.

Figure 7: Continuous time lapse HPICM imaging of stereocilia bundle. (**A**) An overview of an inner hair cell bundle from P5 rat showing distinct shorter row stereocilia. (**B**) Time lapse imaging of the region of interest indicated in (A) throughout six hours. Note that, in contrast to a typical patch camp experiment, the hair cells show no signs of deterioration for several hours in vitro. This is due to careful dissection and the absence of any mechanical disturbances to the cell.

Figure 8: Common artefacts while imaging with HPICM. (**A**) Effect of a too low setpoint. Low-

resolution HPICM images of the same live inner hair cell bundles in P3 mice acquired with setpoint 0.05% (left) and 0.07% (right). Notice a white dot noise that disappears with higher setpoint. (**B**) Effect of a too high hop amplitude. White dot noise also appears in an HPICM image of a P7 rat inner hair cell bundle obtained with a large hop amplitude of 5.8 µm (left). This noise disappears when the same bundle is imaged with the hop amplitude of 3.4 µm (right) due to the decrease of vibrations in the system. (**C**) Too low hop amplitude results in colliding of the HPICM probe to the stereocilia and dragging them (arrows on the left panel). Increasing the hop amplitude just enough to "climb over" stereocilia eliminates this artefact (right) but may also increase imaging time, resulting in a noticeable drift (vertical lines in the right panel). Stereocilia bundle of a live outer hair cell from P7 rat. (**D**) Too high setpoint causes a squared shape of stereocilia tips (arrows) in an HPICM image (left), again due to colliding of the nanopipette to the stereocilia. Decreasing setpoint (with simultaneous decrease of the hope amplitude to eliminate white noise) improves the imaging (right). Stereocilia bundle of a live inner hair cell from P6 rat.

Table 1: Typical times of HPICM imaging depending on the size of imaging area and the scanning resolution.

DISCUSSION:
To obtain successful HPICM images, users need to establish a low noise and low vibration system and manufacture appropriate pipettes. We strongly recommend the use of AFM calibration standards to test the stability of the system before attempting to perform any live cell imaging. Once the resolution of the system is tested, users can consider imaging fixed organ of Corti samples to get familiar with the imaging settings before attempting any live cell imaging.

The optimal setpoint for imaging varies between different pipettes, depending on the individual shape of their tips (that is unknown until examined by electron microscopy) and on the amount of dirt attached to the tip, which is also unpredictable. Nanopipettes with an optimal setpoint higher than 7% should be discarded.

During imaging of live cells, the amount of dust and debris in the extracellular solution increases over time. All these particles can end up at the tip of the pipette, causing a reduction in the current and making it impossible to continue scanning the tissue - the image will turn completely white since the feedback will "think" that the nanopipette is always in the vicinity of the sample. If this happens, it is recommended to retract the pipette in Z-axis from that area of the tissue. This retraction could clear the "dirtiness". If the pipette is still dirty, it is necessary to change the pipette and move to a different area of the sample. Then, the user can continue to scan the tissue.

As of today, the most essential limitation of the HPICM is the amount of time required to take an image at high resolution while working with samples with complex topography. Depending on the resolution desired, images can take up to half an hour or more. In images acquired for longer than fifteen minutes, the drift may become evident and specific structures may be shifted and harder to distinguish. This is happening because the living cells are constantly moving or changing their shape over time. To visualize molecular events and changes in cells' structures over time, further developments are needed to optimize the temporal resolution of the HPICM[11].

651
652 The noise of the nanopipette current represents another limitation because it sets the minimal
653 practically achievable setpoint. The current generated by the nanopipette in the solution
654 attenuates quickly (inverse proportional to the cubic distance from the pipette tip), thereby
655 establishing a "sensing volume", beyond which the nanopipette cannot "sense" the surface. We
656 have previously developed a model of this phenomenon and showed that the lateral resolution
657 of the SICM probe is determined by the cross-section of this "sensing volume" with the cell
658 surface, which could be extremely small at low setpoints[25]. This is particularly important for
659 imaging hair cell tip links that have a diameter of ~5 nm[12,33]. On the first glance, the pipettes with
660 smaller inner diameter would result in better resolution of HPICM imaging. This is indeed true
661 for relatively large pipettes (>50 nm). However, decreasing the inner diameter of the nanopipette
662 below ~50 nm results in unproportionally large increase of the pipette noise and, hence, the loss
663 of resolution at low setpoints that are essential for imaging stereocilia bundles. As of today, we
664 do not know how to solve this problem and we are working on finding the proper solution.
665
666 In summary, this paper presents a detailed protocol for the visualization of stereocilia bundles in
667 live mammalian auditory hair cells with HPICM. The biggest advantages of the HPICM are: i) its
668 ability to visualize label-free nanoscale structures at the surface of living cells without touching
669 them; and ii) to probe the function of these structures with patch clamp recordings and/or local
670 nanoscale delivery of mechanical or chemical stimuli. To the best of our knowledge, these
671 advantages are unique to HPICM. Of course, there are some disadvantages. First, due to
672 limitations on the height of the structures to be imaged, HPICM may not be suitable for imaging
673 extremely tall structures, such as stereocilia bundles of the vestibular hair cells in the mammalian
674 ampullae. Second, HPICM is still developing and further improvements in the speed and
675 resolution of imaging are needed. However, the physical principles of HPICM and our own
676 experience suggest that it is possible. We do believe that HPICM will provide unique data on the
677 function of individual protein complexes at the stereocilia surface.
678

685

686 **DISCLOSURES:**
687 The authors have no competing interests.
688

689 **REFERENCES:**
690

691 1.   Beurg, M., Fettiplace, R., Nam, J. H., Ricci, A. J. Localization of inner hair cell
692 mechanotransducer channels using high-speed calcium imaging. *Nature Neuroscience*. **12** (5),
693 553-558 (2009).
694 2.   Effertz, T., Becker, L., Peng, A. W., Ricci, A. J. Phosphoinositol-4,5-bisphosphate regulates

695   auditory hair-cell mechanotransduction-channel pore properties and fast adaptation. *The*
696   *Journal of Neuroscience : the Official Journal of the Society for Neuroscience*. **37** (48), 11632-
697   11646 (2017).

698   3.   Peng, A. W., Gnanasambandam, R., Sachs, F., Ricci, A. J. Adaptation independent
699   modulation of auditory hair cell mechanotransduction channel open probability implicates a role
700   for the lipid bilayer. *The Journal of Neuroscience : the Official Journal of the Society for*
701   *Neuroscience*. **36** (10), 2945-2956 (2016).

702   4.   Engström, H., Engström, B. Structure of the hairs on cochlear sensory cells. *Hearing*
703   *research*. **1** (1), 49-66 (1978).

704   5.   Conchello, J.-A., Lichtman, J. W. Optical sectioning microscopy. *Nature Methods*. **2** (12),
705   920-931 (2005).

706   6.   Sigal, Y. M., Zhou, R., Zhuang, X. Visualizing and discovering cellular structures with super-
707   resolution microscopy. *Science*. **361** (6405), 880-887 (2018).

708   7.   Wäldchen, S., Lehmann, J., Klein, T., van de Linde, S., Sauer, M. Light-induced cell damage
709   in live-cell super-resolution microscopy. *Scientific Reports*. **5** , 15348 (2015).

710   8.   Pickles, J. O., Comis, S. D., Osborne, M. P. Cross-links between stereocilia in the guinea pig
711   organ of Corti, and their possible relation to sensory transduction. *Hearing Research*. **15** (2), 103-
712   112 (1984).

713   9.   Furness, D. N., Hackney, C. M. Cross-links between stereocilia in the guinea pig cochlea.
714   *Hearing Research*. **18** (2), 177-188 (1985).

715   10.   Jacobs, R. A., Hudspeth, A. J. Ultrastructural correlates of mechanoelectrical transduction
716   in hair cells of the bullfrog's internal ear. *Cold Spring Harbor Symposia on Quantitative Biology*.
717   **55** , 547-561 (1990).

718   11.   Goodyear, R. J., Marcotti, W., Kros, C. J., Richardson, G. P. Development and properties of
719   stereociliary link types in hair cells of the mouse cochlea. *The Journal of Comparative Neurology*.
720   **485** (1), 75-85 (2005).

721   12.   Kachar, B., Parakkal, M., Kurc, M., Zhao, Y., Gillespie, P. G. High-resolution structure of
722   hair-cell tip links. *Proceedings of the National Academy of Sciences of the United States of*
723   *America*. **97** (24), 13336-13341 (2000).

724   13.   Vélez-Ortega, A.C., Freeman, M. J., Indzhykulian, A. A., Grossheim, J. M., Frolenkov, G. I.
725   Mechanotransduction current is essential for stability of the transducing stereocilia in
726   mammalian auditory hair cells. *eLife*. **6**, 1-22 (2017).

727   14.   Ivanchenko, M. V et al. Serial scanning electron microscopy of anti-PKHD1L1 immuno-
728   gold labeled mouse hair cell stereocilia bundles. *Scientific Data*. **7** (1), 182 (2020).

729   15.   Hadi, S., Alexander, A. J., Vélez-Ortega, A. C., Frolenkov, G. I. Myosin-XVa controls both
730   staircase architecture and diameter gradation of stereocilia rows in the auditory hair cell
731   bundles. *Journal of the Association for Research in Otolaryngology : JARO*. **21** (2), 121-135 (2020).

732   16.   Metlagel, Z. et al. Electron cryo-tomography of vestibular hair-cell stereocilia. *Journal of*
733   *Structural Biology*. **206** (2), 149-155 (2019).

734   17.   Langer, M. G. et al. Mechanical stimulation of individual stereocilia of living cochlear hair
735   cells by atomic force microscopy. *Ultramicroscopy*. **82** (1-4), 269—278 (2000).

736   18.   Dufrêne, Y .F. Towards nanomicrobiology using atomic force microscopy. *Nature Reviews*
737   *Microbiology*. **6** (9), 674-680 (2008).

738   19.   Putman, C. A., van der Werf, K. O., de Grooth, B. G., van Hulst, N. F., Greve, J.

Viscoelasticity of living cells allows high resolution imaging by tapping mode atomic force microscopy. *Biophysical journal*. **67** (4), 1749-1753 (1994).

20.   Gavara, N., Chadwick, R. S. Noncontact microrheology at acoustic frequencies using frequency-modulated atomic force microscopy. *Nature Methods*. **7** (8), 650-654 (2010).

21.   Cartagena-Rivera, A. X., Van Itallie, C. M., Anderson, J. M., Chadwick, R. S. Apical surface supracellular mechanical properties in polarized epithelium using noninvasive acoustic force spectroscopy. *Nature Communications*. **8** (1), 1030 (2017).

22.   Katsuno, T. et al. TRIOBP-5 sculpts stereocilia rootlets and stiffens supporting cells enabling hearing. *JCI Insight*. **4** (12) (2019).

23.   Hansma, P. K., Drake, B., Marti, O., Gould, S. A., Prater, C. B. The scanning ion-conductance microscope. *Science*. **243** (4891), 641-643 (1989).

24.   Korchev, Y. E. et al. Specialized scanning ion-conductance microscope for imaging of living cells. *Journal of Microscopy*. **188** (Pt 1), 17-23 (1997).

25.   Shevchuk, A. I. et al. Imaging proteins in membranes of living cells by high-resolution scanning ion conductance microscopy. *Angewandte Chemie (International ed in English)*. **45** (14), 2212-2216 (2006).

26.   Novak, P. et al. Nanoscale live-cell imaging using hopping probe ion conductance microscopy. *Nature Methods*. **6** (4), 279-281 (2009).

27.   Vélez-Ortega, A. C., Frolenkov, G. I. Visualization of live cochlear stereocilia at a nanoscale resolution using hopping probe ion conductance microscopy. *Methods in Molecular Biology*. **1427** , 203-221 (2016).

28.   Gu, Y. et al. High-resolution scanning patch-clamp: new insights into cell function. *FASEB Journal : Official Publication of the Federation of American Societies for Experimental Biology*. **16** (7), 748-750 (2002).

29.   Frolenkov, G. I. et al. Single-channel recordings from the apical surface of outer hair cells with a scanning ion conductance probe. *Association for Research in Otolaryngology*. Abs. 444, (2004).

30.   Sánchez, D. et al. Noncontact measurement of the local mechanical properties of living cells using pressure applied via a pipette. *Biophysical Journal*. **95** (6), 3017-3027 (2008).

31.   Korchev, Y. E., Negulyaev, Y. A., Edwards, C. R., Vodyanoy, I., Lab, M. J. Functional localization of single active ion channels on the surface of a living cell. *Nature Cell Biology*. **2** (9), 616-619 (2000).

32.   Shevchuk, A. et al. Angular approach scanning ion conductance microscopy. *Biophysical Journal*. **110** (10), 2252-2265 (2016).

33.   Furness, D. N., Katori, Y., Nirmal Kumar, B., Hackney, C. M. The dimensions and structural attachments of tip links in mammalian cochlear hair cells and the effects of exposure to different levels of extracellular calcium. *Neuroscience*. **154** (1), 10-21 (2008).
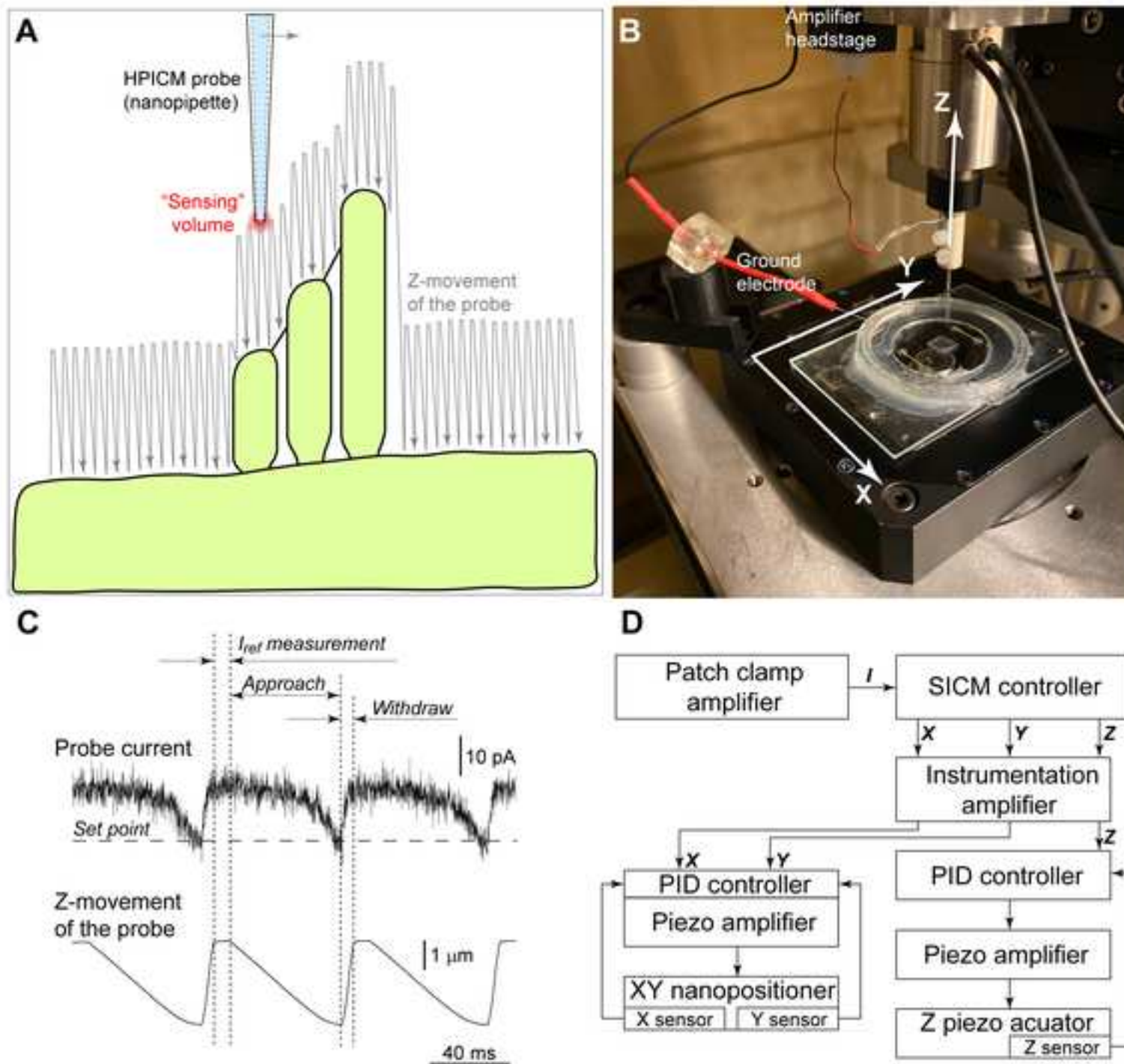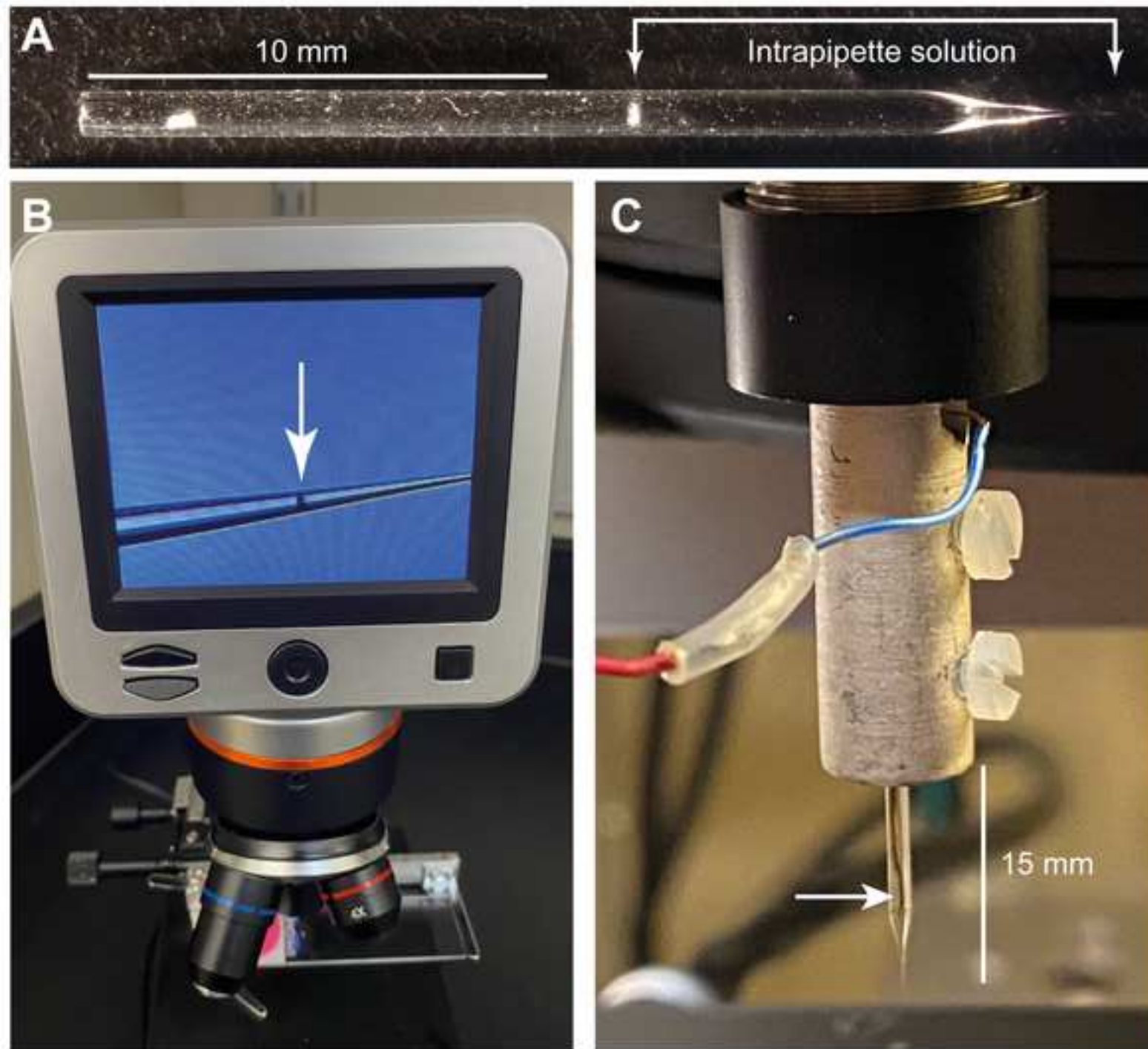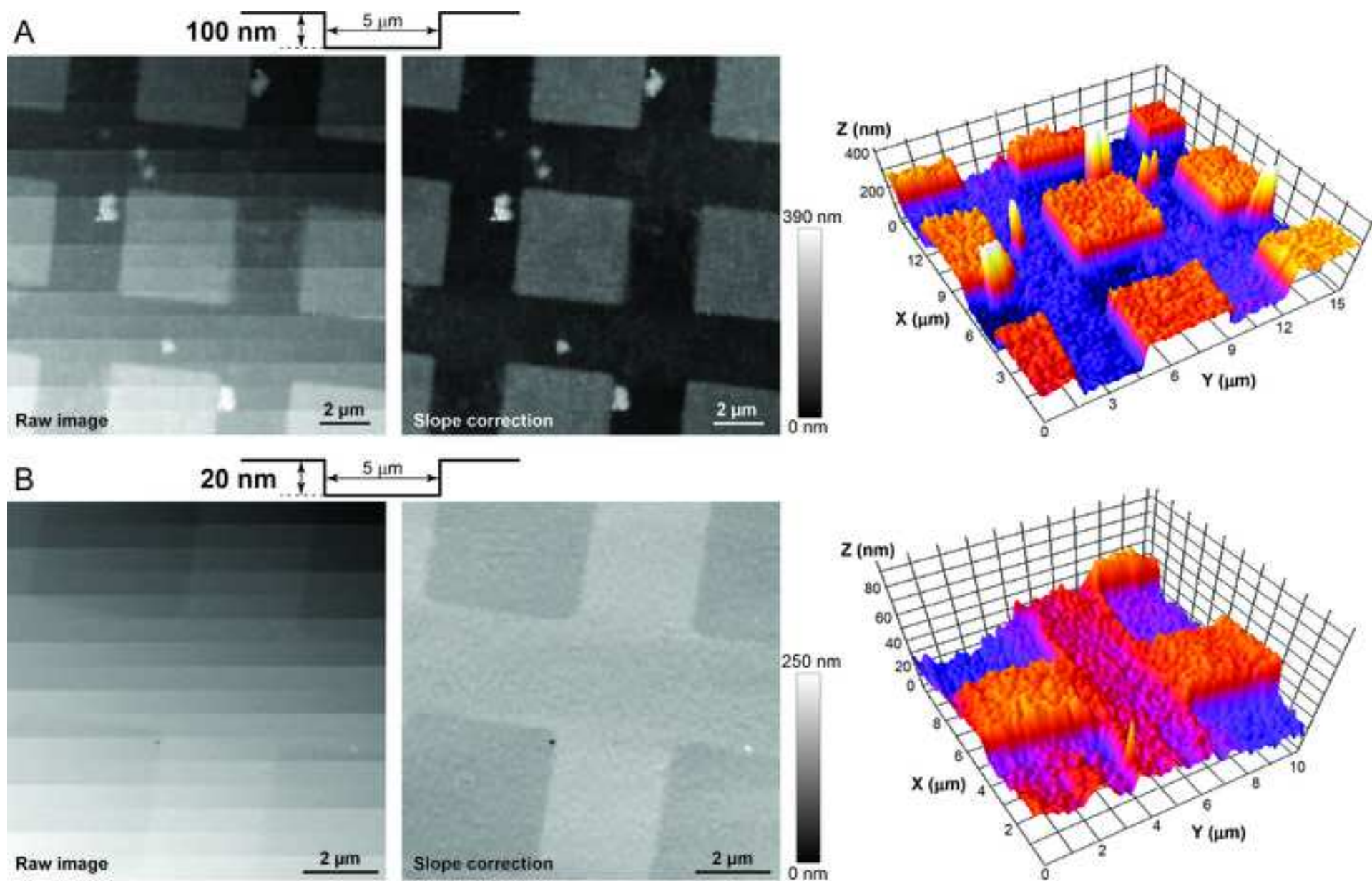
A

HPICM probe
(nanopipette)

"Sensing"
volume

Z-movement
of the probe

B

Amplifier
headstage

Z

Ground
electrode

Y

X

C

I_{ref} measurement

Approach

Withdraw

Probe current

10 pA

Set point

Z-movement
of the probe

1 μm

40 ms

D

| Patch clamp amplifier | I → | SICM controller |

X   Y   Z

Instrumentation
amplifier

Z

X   Y

PID controller   PID controller

Piezo amplifier   Piezo amplifier

XY nanopositioner   Z piezo acuator

X sensor | Y sensor   Z sensor

A 10 mm Intrapipette solution

B

C 15 mm

Figure 3

A — Flexible glass fibers

B — Dental floss, Double cover slip, Tungsten wires; Stria vascularis, Hair cells, Spiral limbus

Scanning Electron Microscopy
(fixed & dried cells)

Hopping Probe Ion Conductance Microscopy
(live cells)

Figure 7

Figure 8

Table 1

Resolution	Image area (μm)	Lateral Resolution (nm)	Time per image (minutes)
Low	20×20	≥300	≤20
Low	10×10	≥156	≤15
Low	5×5	≥75	≤4
High	20×20	≤200	≤20
High	10×10	≤110	≤15
High	5×5	≤55	≤4

Resolution	Image area (μm)	Lateral Resolution (nm)	Time per image (minutes)

Table of Materials

Name of Material/ Equipment	Company	Catalog Number	Comments/Description
Analog oscilloscope	B&K Precision	2160C	Analog oscilloscope for real-time monitoring of nanopipette current and Z-axis approach
AFM calibration standards	TED PELLA Inc	HS-100MG; HS-20MG	These 100 and 20 nm calibration standards are used to test the performance of HPICM system
Benchtop vibration Isolator	AMETEK/TMC	Everstill K-400	Active vibration isolation
Borosilicate glass capillaries	World Precision Instruments (WPI)	1B100F-4	Borosilicate glass capillaries for the nanopipettes
D-(+)-Glucose	Sigma-Aldrich	G8270	To be added to the bath solution to adjust osmolarity
Digitizer	National Instruments Corporation	PCI-6221	Multi-channel input/output digitizer
Fast analog Proportional-Integral-Derivative (PID) control for Z movement	Standford Research Systems	SIM900, SIM960, SIM980	Instrumentation modules integrated in an external PID controller for Z movement. It requires a fast response that is usually not implemented in commercial piezo amplifiers.
Faraday cage	AMETEK/TMC	Type II	Required to shield electromagnetic interference
Glass bottom dish	World Precision Instruments (WPI)	FD5040-100	Used as the dish for the chamber for the tissue
Hanks' Balanced Salt Solution (HBSS)	Gibco, Thermo Fisher Scientific	14025092	Extracellular (bath) solution
Instrumentation amplifier	Brownlee Precision	Model 440	Instrumentation amplifier provides required offsets, filtering, and secondary magnification or attenuation
Laser-based micropipette puller	Sutter Instrument	P-2000/G	Micropipette puller to fabricate the nanopipettes. Laser is needed for sharp quartz pipettes.

Lebovitz's L-15, without phenol red	Gibco, Thermo Fisher Scientific	21083027	Extracellular (bath) solution
Micromanipulator	Scientifica	PatchStar	Used for "course" positioning of the Z piezo actuator
Microscope	Nikon	Eclipse TS100	Inverted optical microscope
Patch amplifier	Molecular Devices	Axopatch 200B	The patch clamp amplifier measures the current through the nanopipette
Piezo amplifier (XY axes)	Physik Instrumente (PI)	E-500.00, E-505.00, E-509.C2A	Amplification and PID control for XY piezo translation stage
Piezo amplifier (Z axis)	Piezosystem jena	ENT 400 & 800	Custom amplifier consisting of ENT 400 power supply and two ENT 800 amplifiers in parallel to achieve max current of 1.6 nA
Plastic Coverslips	TED PELLA Inc	26028	Used in the fabrication of the chambers for the tissue
SICM controller & software*	Ionscope, UK (ionscope.com)	N/A	Custom controller based on SBC6711 digital signal processing board from Innovative Integration Ltd
Silicone elastomer (Sylgard)	World Precision Instruments (WPI)	SYLG184	Used to attach the flexible glass fibers to the chamber for the tissue
Silicon glue	The Dow Chemical Company	734	Used to glue the different parts of the chamber for the tissue
Tungsten rod	A-M Systems	717500	Used for holding the dental floss strands in the chamber for the tissue
XY piezo nanopositioner	Physik Instrumente (PI)	P-733.2DD	XY translation stage with capacitive sensors
Z piezo nanopositioner	Piezosystem jena	RA 12/24 SG	Ring piezoactuator with a strain gage sensor

*Ionscope does not sell separate SICM controllers anymore. There are few other commercial systems: NX12-Bio and NX10 SICM,

Park Systems, Korea and SICM modules from ICAPPIC Limited, UK (icappic.com). All these systems are based on the original HPICM principles. However, imaging stereocilia bundles in the hair cells requires several custom modifications that are technically challenging (or even impossible) in the closed "ready-to-go" systems such as Ionscope or NX12-Bio/NX10. Currently, there is only one modular system (ICAPPIC) that has the flexibility to suit any SICM/HPICM experiment but requires some component integration.

University of Kentucky

Department of Physiology
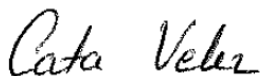College of Medicine

November 30, 2020

Vineeta Bajaj, Ph.D.
Review Editor
JoVE

Dear Dr. Bajaj:

Enclosed please find the revised manuscript JoVE62104, *"Stereocilia Bundle Imaging with Nanoscale Resolution in Live Mammalian Auditory Hair Cells"*. We appreciate the positive and very constructive comments of the reviewers and believe that we have made all necessary changes. Below we provide a point-by-point response to each one of the issues raised by the Editor and the Reviewers. We also uploaded a version of the manuscript with all changes highlighted in blue.

We thank you for your consideration of our manuscript.

Sincerely,

A. Catalina Vélez-Ortega, PhD
Assistant Professor of Physiology

Gregory I. Frolenkov, Ph.D.
Professor of Physiology

see blue.

Lab: Physiology – Room MS-617, 800 Rose St, Medical Science Building | Lexington, KY 40536-0298 | 859-323-8730

An Equal Opportunity University

Editorial comments:

1. Please take this opportunity to thoroughly proofread the manuscript to ensure that there are no spelling or grammar issues. The JoVE editor will not copy-edit your manuscript and any errors in the submitted revision may be present in the published version.

Reply: Done.

2. Please rephrase the Short Abstract/Summary to clearly describe the protocol and its applications in complete sentences between 10-50 words: "Here we present a protocol …"

Reply: Done.

3. Please ensure for in-text formatting, corresponding reference numbers should appear as numbered superscripts after the appropriate statement(s).

Reply: Done.

4. JoVE cannot publish manuscripts containing commercial language. Please remove all commercial language from your manuscript and use generic terms instead. All commercial products should be sufficiently referenced in the Table of Materials and Reagents.
For example: Ionscope, UK (ionscope.com), NX12-Bio and NX10 SICM, 137 Park Systems, Korea; and SICM modules from ICAPPIC Limited, UK (icappic.com), (World Precision Instruments, Inc., Saratosa, FL), 3M, St. Paul, MN, (The Dow Chemical Company, Alberta, Canada), AFM (Ted Pella), Sylgard, etc.

Reply: We have removed mentioning of the companies and their products from the text of the manuscript.

5. Please include an ethics statement before your numbered protocol steps, indicating that the protocol follows the animal care guidelines of your institution.

Reply: Done.

6. We cannot have paragraphs of text in the protocol section. Please move lines 133-166 to the introduction section instead.

Reply: Done.

7. Please include volume and concentrations throughout the protocol.

Reply: Done.

8. Please ensure that all text in the protocol section is written in the imperative tense as if telling someone how to do the technique (e.g., "Do this," "Ensure that," etc.). The actions should be described in the imperative tense in complete sentences wherever possible. Avoid usage of phrases such as "could be," "should be," and "would be" throughout the Protocol. Any text that cannot be written in the imperative tense may be added as a "Note." However, notes should be concise and used sparingly.

Reply: Done.

9. Please ensure you answer the "how" question, i.e., how is the step performed?

Reply: Done.

10. There is a 10-page limit for the Protocol, but there is a 3-page limit for filmable content. Please

highlight 3 pages or less of the Protocol (including headings and spacing) that identifies the essential steps of the protocol for the video, i.e., the steps that should be visualized to tell the most cohesive story of the Protocol.

Reply: Essential steps in the protocol for the video are highlighted in yellow – they occupy less than two pages total.

11. Please obtain explicit copyright permission to reuse any figures from a previous publication. Explicit permission can be expressed in the form of a letter from the editor or a link to the editorial policy that allows re-prints. Please upload this information as a .doc or .docx file to your Editorial Manager account. The Figure must be cited appropriately in the Figure Legend, i.e. "This figure has been modified from [citation]."

Reply: N/A - None of the figures of this manuscript were previously published.

12. Please do not abbreviate the journal titles in the reference section.

Reply: Corrected.

13. Figure 2: Please hide or remove the commercial term.

Reply: Done.

14. Please sort the materials table in alphabetical order.

Reply: Done.

Reviewer #1

Major Concerns:

1. Please give more general information on the technique in the protocol's introduction (lines 147-159). For example, indicate who defines the setpoint and how it is predefined (line 152). Please describe what is considered as an "imaging point" and indicate how big it is (lines 154-156). Please indicate the speed at which the pipette retracts from the sample (line 154). Please explain why the sample is moved instead of the pipette. Is this relevant to the protocol? How is the sample's movement controlled? (line 155). Please indicate how the sample size is determined.

Reply: We have now indicated that the setpoint is defined by the user (line 136). We have also described acquisition of the imaging point as follows: "…the system saves Z value … as the height of the sample, together with X and Y coordinates…" (lines 136-138). We are confused by the reviewer's question about the size of the imaging point. Since piezo actuators can move the nanopipette with a single nanometer precision or even better, the user may set a sub-nanometer pixel size during acquisition of HPICM images. Yet, this "instrumentation" pixel size will have nothing to do with the actual resolution. Throughout the paper, we discuss in detail all the factors that affect the resolution and, therefore, determine a reasonable pixel size that the operator has to choose. Practical values are shown in Table 1.

We have also specified that the speed at which the pipette retracts from the sample is also user-defined and provided the typical range of this speed (lines 138-139). Finally, we described the benefits of pipette versus sample movement in X-Y direction (lines 142-147) and indicated that "the HPICM probe and the specimen stage are moved in Z and X-Y axes by the calibrated feedback-controlled piezo actuators that have an accuracy of a single nanometer or better" (lines 157-158).

2. Please indicate how the calibration sample is attached to the chamber (line 229. Step 3.1).

Reply: Following the Reviewer's comment, we have explained that the calibration sample is attached to the chamber with silicon glue in Step 3.1.

3. Please indicate how the ground electrode is secured to the chamber (line 231. Step 3.4).

Reply: We have clarified in Step 3.3 that the ground electrode has its own magnetic holder that can be position close to the stage to allow the immersion of the electrode in the bath solution. We also labeled it on the Figure 1B.

4. Please define "hop amplitude" in line 239. This seems like a critical concept that is not explained nor defined. In line 245, the authors state that "the hop amplitude can be decreased significantly after obtaining the low-resolution images and determining the highest features within the imaging region." Please explain the relationship between hop amplitude and image resolution.

Reply: As suggested by the Reviewer, in Step 3.8, we have defined the hop amplitude as the amplitude of nanopipette retraction during scanning of the sample. We have also explained that "a smaller hop amplitude allows faster scanning, which is preferred for high resolution imaging due to diminished effects of the drifts and decreased vibration".

5. Please explain how the center of the calibration standard is identified (step 3.5).

Reply: We have explained in Step 3.5 that the nanopipette is positioned over with the center of the calibration sample with patch clamp micromanipulator under visual inspection. We also indicated in this step that, in case of the organ of Corti explants, it is possible navigate the pipette more precisely by observing the tissue and the pipette with an inverted microscope.

6. Please indicate how the chambers are stored and whether they are kept sterile or sterilized before used (step 4).

Reply: We have added the Step 4.3.4 as following, "Place the chamber upside down on a filter paper to let it dry until next experiment. The chambers do not need to be sterilized, unless culturing of the organ of Corti is planned after the imaging."

7. Please indicate how the organ of Corti explants are attached to the custom-build chambers (line 285, Step 5).

Reply: We have explained in Step 5, that the organ of Corti explants are secured under either two flexible glass pipettes or two dental floss strands. This is also shown in Figure 4A and 4B, correspondingly.

8. Please indicate the volume of bath solution added the tissue-containing chambers for image acquisition (line 288, step 5)

Reply: Done. The volume is 4 mL.

9. In line 292, the authors recommend securing the chamber to the HPICM stage to minimize sample drifts. And in line 315, the authors recommend spending less than 15 minutes when imaging a whole hair bundle to minimize the effect of the drift due to the constant movement of living cells over time. A distinction between stage and sample drift would help understand the drift' importance and how to minimize it. Please explain and discuss the differences between the drifts indicated in line 292 and line 315.

Reply: We clarified our terminology in step 6.1 and indicated that the chamber is firmly secured to minimize its drift in X and Y axes. In step 6.9, we are now using a different terminology, "Keep in mind that the hair cell bundles in the live tissue are not still but may change their orientation, for example, due to shape changes in the underlying supporting cells. Therefore, the images may exhibit movement artefacts if the image acquisition is too slow". Usually, "chamber drift" and "cell movement" artefacts

produce different distortions in HPICM images, since chamber drift affects the whole image while cell movements occur only in a group of the cells.

10. Please explain how to check and assure stability in the system (line 295. Step 6.3).

Reply: We have re-phrased this step (now 6.4) as follows, "Check if the system is stable with a setpoint of 0.5% or lower by recording the real-time current and Z positioning signal on the oscilloscope (as in Figure 1C). If the Z signal is not stable, replace the nanopipette."

11. Please explain why the noise appears as white dots in the images acquired at low setpoint or high hop amplitude. Is there a way to differentiate between noise coming from debris and noise coming from a low setpoint or a high hop amplitude?

Reply: We have now described it in the step 7.3: "While obtaining images with HPICM, small fluctuations in the nanopipette current can lead to the nanopipette stopping far from the surface of the sample, especially with low setpoints. It results in the appearance of small white dots in the image as seen in Figure 8A, left." We also re-phrased this explanation in the Representative Results: "with a very low setpoint, the system might interpret small fluctuations in the current as encountering the cell surface and this will lead to the "white dot" noise in the image (Figure 8A)." This noise is indistinguishable from the one occurring when the nanopipette encounter a floating piece of debris during its approach to the sample and, therefore, they both filtered out in the same way during post-processing (see new section 7).

12. Please define "sensing volume" in line 461.

Reply: Following Reviewer's comment, we have explained it as follows, "The current generated by the nanopipette in the solution attenuates quickly (inverse proportional to the cubic distance from the pipette tip), thereby establishing a "sensing volume", beyond which the nanopipette cannot "sense" the surface. We have previously developed a model of this phenomenon and showed that the lateral resolution of the SICM probe is determined by the cross-section of this "sensing volume" with the cell surface, which could be extremely small at low setpoints[25]."

13. Please explain the relationship between the setpoint, pipette diameter, resolution, and noise.

Reply: A special paragraph in the Discussion is dedicated to this (lines 569-581). "The noise of the nanopipette current represents another limitation, since it sets the minimal practically achievable setpoint. The current generated by the nanopipette in the solution attenuates quickly (inverse proportional to the cubic distance from the pipette tip), thereby establishing a "sensing volume", beyond which the nanopipette cannot "sense" the surface. We have previously developed a model of this phenomenon and showed that the lateral resolution of the SICM probe is determined by the cross-section of this "sensing volume" with the cell surface, which could be extremely small at low setpoints[25]. This is particularly important for imaging hair cell tip links that have a diameter of ~5 nm[12,32]. On the first glance, the pipettes with smaller inner diameter would result in better resolution of HPICM imaging. This is indeed true for relatively large pipettes (>50 nm). However, decreasing the inner diameter of the nanopipette below ~50 nm results in unproportionally large increase of the pipette noise and, hence, the loss of resolution at low setpoints that are essential for imaging stereocilia bundles. As of today, we do not know how to solve this problem and we are working on finding the proper solution."

14. Please indicate the band pass filter used for data acquisition and how this may affect the experimental outcome.

Reply: We have re-phrased step 6.4 as follows, "Check if the system is stable with a setpoint of 0.5% or lower by recording the real-time current and Z positioning signal on the oscilloscope (as in Figure 1C). If Z signal is not stable, try to decrease the cutoff frequency of the low-pass filter of the patch clamp amplifier. However, it cannot be lower than the response time of Z piezo actuator (to avoid pipette collision with the sample due to delayed current readings). In practice, we have found that 5 kHz setting of this filter is optimal. It is better to replace the nanopipette, if Z-signal is still unstable."

15. Several materials and equipment were not listed in the Table of Materials. Please include the information on the puller and capillaries used to fabricate the pipettes, the material used to prepare the custom-built chambers, the calibration standards, and the software used to acquire the experimental data and perform the processing.

Reply: Following the Reviewer's comment, we have updated our Table of Materials.

Minor Concerns:

16. Please indicate the preferred direction of the HPICM probe in figure 1A.

Reply: We have indicated the preferred left-to-right direction of scanning with an arrow in Figure 1A. We have described it in the figure legend as follows, "Illustrated hop amplitude would work for left-to-right scanning (from smallest to a tallest stereocilium, indicated by an arrow). However, it is too small for right-to-left scanning when the pipette meets the tallest stereocilium first."

17. In Figure 3-7, please indicate the meaning of the grayscale (um).

Reply: We are again confused by the comment. All our HPICM images in Figure 3, Figure 5 (B and C), Figure 6 (B, D, and F) and Figure 7 do have grayscale calibration bars. However, Figure 4 show optical images, while Figure 5A, Figure 6 (A, C, and E) show scanning electron microscopy images. In all of them, grayscale cannot be meaningfully interpreted in a quantitative way. Perhaps, the Reviewer wanted us to mention that, in all HPICM images, the greyscale of a pixel indicates the height of the sample at that point. We have mentioned it now in the figure legends.

18. Please label the glass capillaries in figure 4A and wires in figure 4B.

Reply: Done

19. Please indicate the outer and inner hair cells in figure 5.

Reply: Done

20. In Figure 7 and text, please clarify if the sample was constantly imaged for 6 hours or one image was taken every hour.

Reply: We have clarified that the sample was continuously imaged for 6 hours.

Reviewer #2:

Major Concerns:

1. The authors describe the advantages of their protocol/technique, but what are the disadvantages? And drawbacks. Please discuss comprehensively.

Reply: We would like to thank the reviewer for this particular comment. We now discuss disadvantages in many places of the manuscript: i) an original SICM requirement of a relatively flat surface that was alleviated by HPICM (lines 110-113); ii) the requirement for personnel with the electrophysiological background (lines 170-174); iii) relatively slow imaging with HPICM (lines 561-567); and yet not optimal resolution of HPICM (lines 569-581). To summarize major advantages and disadvantages, we re-phrased the last paragraph of the Discussion as follows: "The biggest advantages of the HPICM are: i) its ability to visualize label-free nanoscale structures at the surface of living cells without touching them; and ii) to probe the function of these structures with patch clamp recordings and/or local nanoscale delivery of mechanical or chemical stimuli. To the best of our knowledge, these advantages are unique to HPICM. Of course, there are some disadvantages. First, due to limitations on the height of the structures to be imaged, HPICM may not be suitable for imaging extremely tall structures, such as stereocilia bundles of the vestibular hair cells in the mammalian ampullae. Second, HPICM is still developing and further

improvements in the speed and resolution of imaging are needed. However, the physical principles of HPICM and our own experience suggest that it is possible. We do believe that HPICM will provide unique data on the function of individual protein complexes at the stereocilia surface."

2. How difficult, demanding, time and money consuming is it to establish the procedure for a scientist with and without patch clamp experience? Please describe comprehensively in the text.

Reply: Following the reviewer's comment, we have added the approximate cost of materials/equipment in the table of materials. We also clarified in the Introduction that HPICM "integration is relatively easy for any researcher, who is proficient in patch clamping. However, a scientist without proper background would definitely need some training in electrophysiology first." According to our experience, a scientist with a proper background becomes excited very easily by HPICM capabilities, while a scientist without proper background either in electrophysiology or in electrical engineering may have hard time understanding even basic principles of HPICM.

3. I may ask the authors to include a comprehensive section about the analysis and processing of the data to provide a detailed protocol for the visualization of stereocilia bundles as claimed in line 470.

Reply: Done. See entirely new section 7.

Minor Concerns:

Introduction-Section:

4. line 61: Could the authors please describe the local mechanisms that regulate signalling at the tips of stereocilia?

Reply: We are referencing two recent papers (refs #2 and 3) that provide substantial evidence for such local mechanisms regulating mechano-electrical transduction at the tips of stereocilia. The mechanisms themselves are still subject of intense investigation and, therefore, it is hard to speculate about them in the Introduction. In fact, we are developing HPICM technique in order to study these mechanisms.

5. line 108: I am not sure whether an 11-year old publication can be described as "only recently"

Reply: Words "only recently" have been removed.

6. line 128 and lines 283/284: I was wondering about why the technique apparently is limited to maximally 8 days old rodents and hence only allows for analysis of premature hair cells? I think this is also some important information for readers interested in analyses of the inner ear.

Reply: We have clarified that "older hair cells are more susceptible to the damage during dissection and, therefore, cannot be used for hours-long time lapse HPICM imaging" (lines 329-331).

Protocol-Section:

7. The first paragraph of the protocol-section addressed the equipment and the technique as such. To increase clarity, I was wondering whether it was possible to introduce a subheading at that point.

Reply: We have moved this paragraph to the Introduction.

8. lines 139 (following): The authors describe the need of integrating several components into available recording systems. For non-expert readers, it may be beneficial to briefly describe those component, to highlight the difficulties and pitfalls of integration and maybe also to present a schematic of the setup with all components in a Figure (the setup is hard to appreciate from the presentation in Figure 1B in its present form). Is it possible to give approximate costs for the setup and also minimally required time to establish the procedure (let´s say from a working pclamp setup).

Reply: Following the reviewer's comment, we have added the cost for materials/equipment in the Table of Materials. We have also added to the Figure 1 a new panel D, which describes the most essential equipment that needs to be added to a standard patch clamp setup. As to the time required to assemble and troubleshoot the HPICM rig, it is highly variable, depending on qualification and experience of the researcher.

9. line 176: Could the authors please specify the "resonance" expected to increase with the length of pipettes.

Reply: We have clarified in the step 1.2 that "The length of the pipette is crucial because it determines the frequency of the lateral mechanical resonance of the pipette. The longer is the pipette, the lower is the resonant frequency and the harder is to avoid this resonance."

10. Figure 2C: Could you please also give a scale in this image?

Reply: Done.

11. line 180: D-glucose apparently is added to the solution to adjust the osmolarity. Please, give this information also here in the text.

Reply: The Reviewer is correct; glucose was added to adjust osmolarity. This info has been added to the text.

12. line 185: I was wondering, why it is more difficult to remove bubbles from "older" pipettes, as I have not yet noticed this correlation.

Reply: We were also puzzled by this phenomenon since we also never noticed it in the larger pipettes used for patch clamping. Therefore, we have admitted it by saying, "For the reasons that we do not yet understand, it is harder to remove bubbles in the pipettes that have been pulled several hours before the experiment."

13. line 202: Apparently the ideal pipette resistance value range is rather large and between 200 - 400 MΩ. Can the authors maybe precise this (narrow it down) a bit, or is 200 MΩ exactly as good as 400 MΩ.

Reply: There is a compromise that we have explained as follows: "In our experience, the ideal resistance value is between 200 and 400 MΩ. Pipettes with a resistance higher than 400 MΩ might lead to an unstable current due to their small size (< 50 nm inner diameter). On the contrary, pipettes with resistances smaller than 200 MΩ are too large (> 70 nm inner diameter) and would not resolve small features. Its recommended to start imaging with the pipettes of 200 MΩ resistance, as they are easier to manufacture and tend to provide less electrical noise." The exact value depends on what the researcher wants: a stable recording with a worse resolution or a better resolution with the recordings that may be unstable.

14. line 205 "…and will be unable to..": Maybe, the authors could change this to "…impeding resolution of…" or something like that.

Reply: Corrected.

Minimizing sample drifts and vibrations + making custom-built chambers (Sections 2+4)

15. I fully understand that minimizing vibrations/movements of the tissue and the setup are crucial for these kind of recordings. As an electrophysiologist, I was wondering whether a setup optimized for standard patch clamp (as far as vibration is concerned) is suitable or whether the vibrations even need to be lower. Maybe this is also important information for other readers and should be mentioned in the next (together with highlighting the need for vibration-reduced tables, etc.)

Reply: Again, we thank the Reviewer for the comment. We have clarified that "HPICM setup represents a patch clamp rig with more stringent vibration and drift requirements" (Introduction) and that "a small drift with a speed of less than a micrometer per minute is usually not noticeable in a regular patch clamp setup. Yet, it could produce artefacts of several tens of nanometers in HPICM imaging, which is significantly larger than the resolution of HPICM" (step 7.2).

16. I find the sections on custom-built chambers (Section 2+4) quite difficult to understand and I guess that this may be more easy to understand by means of the video. Nevertheless, the authors should revise these sections (2 + 4) to increase clarity and also show a schematic representation of these custom-built devices.

Reply: We have added additional info (steps) to the Sections 2 and 4 to improve clarity. We have also explained the reason why we are using two types of chambers. "The glass pipette chamber could be sterilized and used for the cultured organs of Corti, while dental floss chamber provides a more secure holding of the sample and a control over stereocilia bundle orientation during mounting."

17. Figure 4: The described components (coverslip, wire, floss, etc.) are difficult to appreciate and should be highlighted in the figure. The cochlear structures are very difficult to see in the image inset.

Reply: We have now labeled the components of the chambers in Figure 4. The goal of the inset, however, is to show the organ of Corti mounting rather than the cochlear structures. Higher magnification would show these structures better but would not show the mounting.

Testing the system's resolution (Section 3)

18. Line 219: Do the authors advise calibration of the system on a daily basis or only once week, month,… (this should be mentioned in the text).

Reply: We apologize for the apparent confusion. HPICM system doesn't need often calibrations, because every axis is driven by a piezo translation stage (or an actuator) with a build-in movement sensor (calibrated during the setup, see new Figure 1D). The rationale for imaging of the AFM standards is to test the stability and the noise of the system and, hence, the practically achievable resolution. We have clarified it now as follows. "We strongly recommend imaging AFM standards (see Materials table) before imaging live cells in order to troubleshoot the system and test its resolution in the X-Z-Y axes."

19. Figures 5, 7B, 8: Insert blank between value and unit above scale bars

Reply: Corrected.

20. line 265: Should it be "of" rather than "off"?

Reply: Corrected

21. line 481: change "advise" to "advice"

Reply: Corrected